Proceedings of the 30th International Cosmic Ray Conference
Rogelio Caballero, Juan Carlos D'Olivo, Gustavo Medina-Tanco,
Lukas Nellen, Federico A. Sánchez, José F. Valdés-Galicia (eds.)
Universidad Nacional Autónoma de México,
Mexico City, Mexico, 2008

Vol. 5 (HE part 2), pages 1539–1542

30TH INTERNATIONAL COSMIC RAY CONFERENCE

Simulated Sensitivity of the ANITA Detector and Relative Sensitivities for Signals Observed Directly and via Reflections

F. WU[1], A. CONNOLLY[2] FOR THE ANITA COLLABORATION[3]
[1]*Dept. of Physics and Astronomy, University of California-Irvine CA 92697*
[2]*Dept. of Physics and Astronomy, University College London, London WC1E 6BT*
[3]*See paper 1219, and special section of these proceedings, for complete author list*
fenfangw@uci.edu

Abstract: The balloon-borne ANITA neutrino telescope completed a successful 35-day flight during the 2006-2007 austral summer. The primary goal of ANITA is to search for evidence of ultra-high-energy neutrinos ($E > 10^{18.5}$ eV) interacting in the Antarctic ice sheets. In this paper, we present preliminary results of the simulated sensitivity of ANITA, incorporating the actual flight path, geographic and vertical temperature dependence of ice, and flight trigger conditions. We also present the relative sensitivity of ANITA to signals reflected from the bottom of Antarctic ice shelves. Reflected events make a significant contribution to ANITA's total sensitivity only if σ_ν is much larger than that predicted in the standard model.

Introduction

ANtarctica Impulsive Transient Array (ANITA) is a long-duration balloon experiment designed to detect ultra-high-energy (UHE) neutrinos produced by the Greisen-Zatsepin-Kuzmin (GZK) process [1, 2]. As UHE neutrinos hit the ice, they interact with the nuclei in the ice and create particle cascades. Because the generated particles in the cascade move faster than the speed of light in the ice, Cherenkov radiation is produced. At radio frequencies the Cherenkov radiation is coherent, which makes it promising to detect these distinctive short duration pulses, called Askaryan pulses [3].

Since the predicted GZK neutrino flux is very small and the neutrino-nucleon cross section is tiny [4], a detector with large effective volume is required. Antarctica is a very promising place to detect the neutrino-nucleon interactions because 99% of the continent is covered by ice which is nearly transparent at radio-frequencies and the radio background noise is relatively low. ANITA takes advantage of these favorable conditions. The payload consists of 32 dual-polarization (vertical and horizontal linear) quad-ridged horn antennas, which observed Antarctic ice from an altitude of $\sim$37 km for almost 35 days beginning December 15, 2006. ANITA completed 3.5 orbits while observing on average about 2×10^6 km^3 ice at any given time.

ANITA was mainly designed to detect neutrinos traveling in the horizontal direction. The signals from the upper part of the Cherenkov cone would be nearly horizontal after refraction at the ice-air surface and can reach the far away ANITA payload. A downward-going neutrino would produce a Cherenkov signal whose cone is aimed entirely toward the bottom of the ice and would normally be undetectable. However, ANITA might still be able to detect neutrinos traveling downward when it is in view of ice shelves (large ice structure floating on sea-water) where the ice is thinner with a smooth surface underneath. In this case the signals could be reflected from the water-ice boundary and reach the payload.

Simulations

Two independent simulation programs have been used by the ANITA collaboration [5]. In this paper, the UCL based program (icemc) is discussed. The

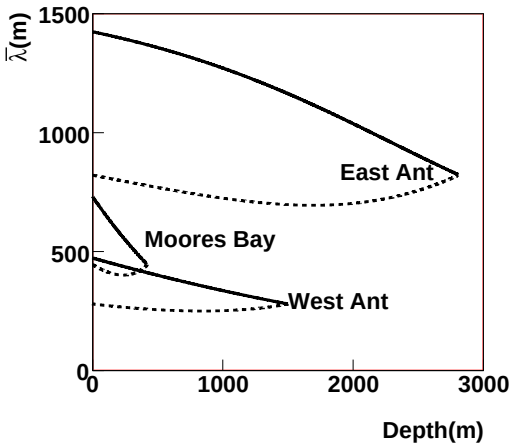

Figure 1: Representative values for field attenuation length $\bar{\lambda}$ plotted as a function of depth for various geographical locations in Antarctica. Solid lines indicate radio signals that come upward directly from the neutrino interaction point. Dashed lines are for radio signals that first propagate down to the ice bottom and then reflect upward.

icemc simulation models interactions from neutrinos of a specified energy. First a neutrino-nucleon interaction is required to occur in the Antarctic ice volume within the balloon's horizon. Then we find the unique path along which an RF signal would travel from the interaction to the balloon, using Snell's law to trace the signal through ice layers near the ice-air surface. Next, we pick a neutrino direction at random and weight the events to account for absorption of the neutrinos in the earth. Depth-dependent attenuation lengths and indices of refraction in the ice are based on recent South Pole measurements [6].

We find a nominal slope of the ice surface where the signal exits the ice by comparing the relative heights of the ice surface at neighboring points in the BEDMAP model [7]. Large scale changes in the surface tilt are modeled by adding a randomized component to this nominal slope such that the angle between the local slope compared to the nominal slope is $\sim 1^{\circ}$. Small-scale (comparable to the radio wavelengths measured by ANITA) roughness is not included in the icemc aperture calculations. Refracted emission from the ice-air interface is propagated geometrically to the payload where a detailed instrument model of the ANITA detector is used to generate triggered events. Frequency-dependent antenna response is based on the manufacturer's specifications but modified according to lab measurements. In addition, icemc was modified for the actual flight path of ANITA and the system live time was estimated by eliminating time periods in excess of 10 minutes that collected no data.

The icemc simulation accounts for the propagation of neutrinos through the standard atmosphere and the Earth crust, for both charged-current and neutral-current interactions of all neutrino flavors, and for electromagnetic and hadronic showers (LPM effect included). Secondary interactions by the outgoing charged leptons are also included, but are all co-located at the interaction vertex. The radio emission is parameterized by the current theoretical model [8] which has been validated by accelerator measurements [9]. The ice thickness for both sheet and shelf ice is obtained from the BEDMAP compilation of the topographical information [7]. Ref. [10] provides the surface temperature distribution over geographic locations (East Antarctica, West Antarctica Land, Ice Shelves). Due to different temperature and ice thickness, the electromagnetic properties of the plateau and iceshelf are distinct. The field attenuation length for radio propagation depends on the initial depth of the interaction in the ice. Based on the vertical temperature profile of the ice and the measurements obtained at the South Pole [6], a depth-dependent attenuation length ($\bar{\lambda}$), averaged over frequency, is shown in figure 1. The effective attenuation length for direct events decreases with depth of the interaction due to the strong temperature dependence of the attenuation length. Due to the fact that East Antarctica ice sheet is higher and colder, the attenuation length of its ice is much larger than that of West Antarctica (both west land and ice shelves). We view this as conservative because the most recently measured one-way attenuation length in the Ross Iceshelf (shown as Moores Bay in figure 1) is ~ 450 meters at the radio frequencies of interest [11]. The maximum attenuation length can be varied in icemc to help assess systematic uncertainties.

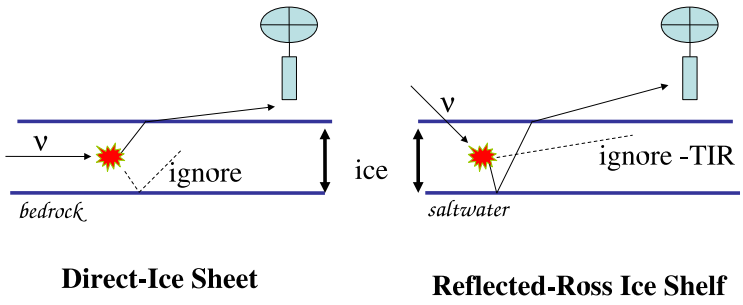

Figure 2: Schematic representation of "direct" (left) events that originate in the ice sheet and "reflected" (right) events which are possible from the Ross Ice Shelf. For the reflected case, the direct ray shown cannot escape due to total internal reflection (TIR).

The experimental trigger is simulated by dividing the signal into four frequency bands, and requiring that 3 of 8 bands, corresponding to the horizontal and vertical polarizations, exceed an effective nominal threshold of 2.3 V_{rms}. During flight, the ambient RFI noise environment changed, so band thresholds were adjusted to maintain a relatively constant trigger rate. If strong RFI at a particular frequency was observed, the threshold of the band containing the RFI was increased. The thresholds were indirectly measured by the scaler rates of each band. A simple linear function that depended on the measured scaler rates was used to adjust the thresholds in the detector simulation program. Also, the simulation implements the "hit pattern" requirements of the trigger.

The amplitude of the signals reflected from the bottom of the ice sheet is greatly attenuated and scattered by the fragmented, rocky bottom and they are typically ignored. However, the bottom of the ice shelf reflects the radio signals with very good fidelity except in regions with crevassing due to sea currents [12]. Signals reflected from the bottom of ice shelves can be observed from a large range of incident angles. Figure 2 describes the overall geometric scheme. The term "direct" refers to signals that propagate directly from the emission region to the air-ice surface and then refract toward ANITA. "Reflected" signals first travel downward and then reflect from the bottom interface.

In order to simulate the reflected events case, the mirror-interaction position is obtained by reflecting the source about the ice bottom. This mirror-interaction point is then treated as a real interaction position, so that we can repeat the modeling process for direct events, with some modifications required. We assume that the ice rock boundary at the bottom of the ice sheet reflects very little power (-30dB) but in contrast the reflected power from the seawater-ice boundary beneath the ice shelves loses very little (-3dB) [11].

Discussion

We present some preliminary results for ANITA effective apertures for a variety of configurations. Figure 3 compares the aperture for the actual flight and trigger conditions with an idealized circular path at $80°$S. It shows that the actual trigger conditions decrease the aperture by a factor of 2 but the large scale surface tilt has little impact on the aperture. We also investigate whether attenuation length and reflections are important for ANITA sensitivity. Figure 4 illustrates the relative impact on aperture for two assumptions on $\bar{\lambda}$ for both direct and reflected events. We find that the aperture for reflected events is $\sim 10\%$ of the aperture of direct events. In addition, the reflected event aperture has a relatively large dependence on the $\bar{\lambda}$.

There remain several areas that would benefit from additional study to evaluate the impact on ANITA's neutrino sensitivity. (a) Small Scale Surface Roughness. The icemc simulation includes large-scale slope variations of the snow surface, but doesn't include the potential impact of surface

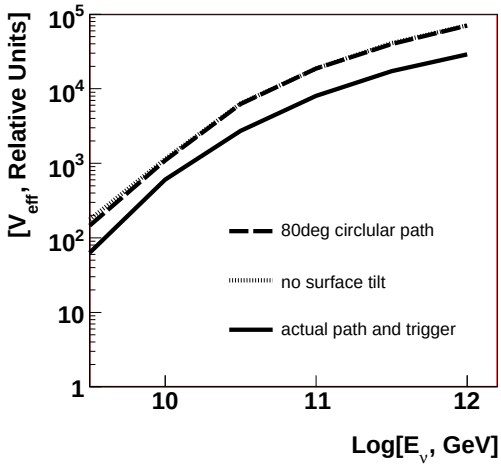

Figure 3: ANITA relative effective apertures averaged over neutrino flavor. The solid curve indicates the actual path of ANITA including trigger and band masks. The other two curves correspond to an idealized circular path at $80°$S and idealized trigger, (dashed) including surface tilt, (dotted) no surface tilt included.

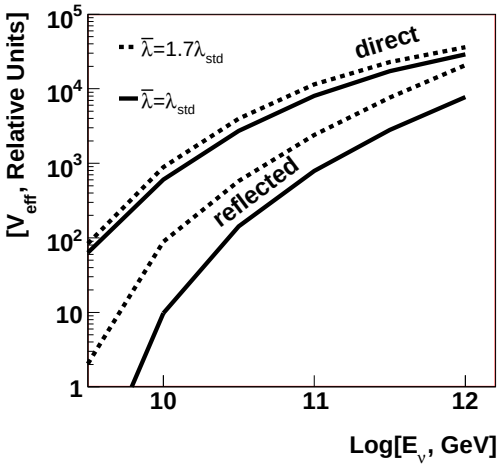

Figure 4: ANITA effective apertures for direct (upper two curves) and reflected events(lower two curves), with two assumptions for attenuation length. The solid curve indicates the nominal attenuation length (λ_{std} given in figure 1). The dashed curve is for $1.7\lambda_{std}$.

microrelief of the Antarctic Ice Sheet. The character and density of the microrelief are continuously changing in response to the surface conditions of wind, temperature, and snow precipitation. (b) Birefringence effects, due to the structure of the ice crystal and asymmetry in the crystal orientation fabric, can alter the time dependence of the Cherenkov pulse by producing a prompt and delayed component [13].

Acknowledgements

This work has been supported by the United States Department of Energy and NASA. We thank the National Science Foundation and Columbia Scientific Balloon Facility for their excellent support.

References

[1] K. Greisen, Phys. Rev. Lett. 16 (1966) 748–750.
[2] G. Z. V.A. Kuz'smin, JETP Letters 4 (1966) 78.
[3] G. Askaryan, JETP 21 (1965) 658.
[4] G. et al., Phys. Rev. D 58 (9) (1998) 093009.
[5] S. B. et al., Phys. Rev. Lett. 96 (17) (2006) 171101.
[6] S. B. et al., J. Glaciology 51 (2005) 433.
[7] M. L. et al., J. of Geophys. Res. 106 (2001) 11335.
[8] J. A.-M. et al., Phys. Rev. D 62 (2000) 063001.
[9] S. et al., Phys. Rev. Lett. 86 (13) (2001) 2802–2805.
[10] http://nsidc.org/data/thermap/.
[11] S. B. et al., these proceedings ID 1163.
[12] C. Neal, J. of Glaciology 24 (1979) 90.
[13] D. B. et al., astro-ph/0703413.